Theor Chem Acc (2010) 125:279–291
DOI 10.1007/s00214-009-0697-7

REGULAR ARTICLE

On the structure, infrared and Raman spectra of the 2:1 cysteine–Zn complex

Martina Kieninger · Oscar N. Ventura

Received: 22 September 2009 / Accepted: 30 October 2009 / Published online: 3 December 2009

Abstract A recent study on the Raman spectrum of the cysteine zwitterion and anion, and the 2:1 $(Cys)_2Zn$ complex was reanalyzed employing B3LYP/6-311++G (3df,2pd) calculations in a simulated water environment. The spectra were rediscussed in light of the apparent incorrect structure determined in the original paper for this complex. The complex turns out to be tetrahedral and tetracoordinated instead of octahedral hexacoordinated, as initially proposed. The calculated Raman spectrum of the complex agrees very well with the experimental data, showing that both the geometrical and electronic structures are well represented. Three metal–ligand bands are found, two of them involving mostly the symmetrical and asymmetrical stretching of the Zn–N and Zn–S bonds. They were measured at 334 and 296 cm^{-1} and calculated at 319 and 249 cm^{-1}, respectively. The third band involves the stretching of Zn–S bonds but also skeletal vibrations of the ligand. This band, measured at 399 cm^{-1} and calculated at 444 cm^{-1}, has been previously assigned incorrectly to a Zn–O bond which does not actually exists since the CO_2^{-1} fragments are located away from the Zn ion.

Keywords Cysteine · Zinc · Metal–ligand bands · Zinc fingers · DFT calculations · Rama spectra

Dedicated to Professor Sandor Suhai on the occasion of his 65th birthday and published as part of the Suhai Festschrift Issue.

M. Kieninger · O. N. Ventura (✉)
Computational Chemistry and Biology Group (CCBG),
Faculty of Chemistry, Detema, Udelar,
C.C. 1154, 11800 Montevideo, Uruguay
e-mail: onv@fq.edu.uy

1 Introduction

The four-aminoacid sequence $(Cys)_2(His)_2$ tightly bound to a Zn^{2+} ion has become known with the name of '*zinc finger*'. Initially used to define a repeated zinc-binding motif with DNA-binding properties in the *Xenopus* transcription factor IIIA, the term 'zinc finger' is now largely used to identify any compact domain stabilized by a zinc ion [1]. It is probably the best studied small domain in proteins [2–6] and a very useful tool for gene manipulation [7].

As in other cases of metal ion binding to proteins, zinc fingers rely on the ability of cysteine to bind to the divalent Zn(II) ion. Cys may form chelate rings with divalent metal ions employing any of its three coordination sites (sulfhydryl, amino and carboxylate sites). Not surprisingly then, the structure of these complexes have been often investigated in the past decades. An important precedent in this sense is the paper by Shindo and Brown [8], where they determined the characteristic IR bands of several possible complexes of cysteine and Zn(II). These experimental data show that the 2:1 Cys–Zn(II) complex occurs through S,N coordination, since the carbonyl absorption occurs in the expected region for uncoordinated $–CO_2^-$. Other studies have pointed out the possibility that the metal is actually coordinated by the terminal S, N and O of both cysteines [9] instead of by the S and N atoms only. Gockel, Vahrenkamp and Zuberbühler used potentiometric titrations of aqueous solutions to study 1:1 and 1:2 Zn complexes of Cys and His. They concluded that the order of stabilities can be explained by the relative strengths of the Zn–S versus Zn–N coordination, charge effects, and chelate ring sizes. Although in this and later publications [10] the authors clearly indicate that Zn(II) is tetracoordinated and that this coordination occurs through the S and N atoms, their initial suggestion about the possibility of O

coordination was used recently as a justification for a tridentate complex as a way to explain the $(Cys)_2Zn^{2-}$ Raman spectrum [11].

Foley and Enescu [11] studied the Raman spectrum of this 1:2 zinc–cysteine complex in aqueous solution and compared it to those of the cysteine zwitterion and cysteine anion in order to characterize specific complexation effects. Their study was based on frequency calculation and normal modes analysis using the B3LYP/6-31+G(d) DFT method. An important discrepancy between their results and our own computational ones, obtained in the framework of other studies, prompted us to study more closely the conclusions of their work. We were able to identify the source of this discrepancy, due to their use of a wrong stereoisomer in the building of the complex for the theoretical studies. As can be seen in their Fig. 1, reoptimized in this work and shown in our own Fig. 1a, while one of the Cys fragments is the correct L-Cys, the other is actually *R*-Cys, allowing then for the construction of such a complex, which we will show is unstable if both L-Cys residues are employed.

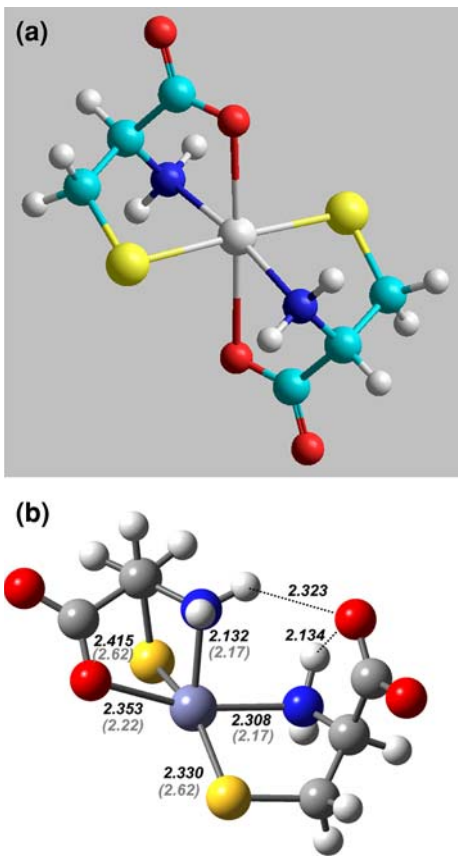

Fig. 1 **a** Optimized structure of (L-Cys)(*R*-Cys)Zn(II)$^{-2}$ as determined by Foley and Enescu [11]. Notice the two different stereoisomers employed (L and *R*). **b** Reoptimized structure at the same B3LYP/6-31+G(d) level, allowing free variation of all geometrical parameters. The values in parenthesis are those determined in Ref. [11] for the symmetric hexacoordinated complex in **a**

In this work we describe the theoretical results obtained at the DFT level for the 2:1 $(L\text{-Cys})_2Zn(II)$ complex and analyze the IR and Raman experimental spectra in terms of the correct structure.

2 Methods

Geometry optimization of the 2:1 Cys–Zn complexes, as well as the monomeric Cys and Cys^{2-} species, were performed in gas phase using the B3LYP [12] DFT method [13], with the 6-31+G(d) and 6-311 ++G(3df,2pd) basis sets (full core was used for the Zn atom instead of pseudopotentials). Optimizations were carried out until all cartesian coordinates were accurate to 10^{-4} Å. B3LYP was used as the DFT method of choice because it is more accurate than similar adiabatically coupled methods like PBE0 [14], notwithstanding the more ab initio formulation of the latter.

Minima were identified analyzing the second derivative matrix calculated analytically and assuring that no negative eigenvalue was present. The Hessian was also employed to calculate IR and Raman frequencies and intensities. In the last case, numerical differentiation of the Hessian with respect to the electric field was performed to obtain the Raman activity for each transition. No anharmonic correction was attempted in this work. Basically three complexes were studied: the closed, tridentate 1:2 complex with a hexacoordinated Zn(II) metal ion, arising from L-Cys and *R*-Cys coordination, as studied by Foley and Enescu [11] (Complex A), the similar closed form complex formed by two L-Cys coordinated cysteines (Complex B), and the open, bidentate Cys tetracoordinated Zn(II) complex where the carboxylates of both proteins do not interact with the metal ion (Complex C).

The gas-phase calculations were complemented by the study of the spectra in a water environment. Th rationale behind this approach is the observed dependence of aminoacid conformations on the liquid environment, especially in the case of the zwitterionic species. For instance, recent work using vibrational absorption, vibrational circular dichroism, Raman scattering, Raman optical activity and NMR has verified that the structure for the alanine dipeptide in aqueous solution is one which is not even stable on the gas phase potential energy surface [15–19]. Similar work was performed on histidine [20], the peptide backbone [21] and methyl lactate [22]. In the latter case one can see even VCD signals due to bound water. A very recent work [23] shows that the zwitterionic species of L-alanine is also much better modeled by adding explicit water molecules, and embedding the cluster within a continuum

model (which then treats the effects due to bulk water). We expect the effect to be much less important for the anion (the most important species in relation to the structure of the complex) but nonetheless significant. Therefore, we sought to include the solvent effects in two different ways. The PCM method of Tomasi and collaborators [24] was used to perform a reaction field calculation using the integral equation formalism model. A continuum solvent environment was used to simulate water (dielectric constant 78.39) and both geometry optimizations and frequency calculations were carried out in this environment. Spectra calculated in this simulated water solvent were then compared to the ones obtained in gas phase.

A similar calculation was performed representing water by 13 discrete water molecules arranged around the anion in the case of cysteinate. The initial positions of the water molecules were obtained from the molecules belonging to the first or second solvation shell in a snapshot of the stabilized droplet obtained from a classical molecular dynamics simulation (Amber force field, 0.833 electrostatic

Table 1 Geometry optimization of the Cys anion and zwitterion at different levels of theory

Parameter	Cys anion						Cys zwitterion			
	B3LYP/6-31+G(d)				B3LYP/6-311++G(3df,2pd)		B3LYP/6-311++G(3df,2pd)		Experimental	
	PCM Ref. [11]	PCM water	Discrete water	Gas phase	PCM water	Gas phase	PCM water	Gas phase	X-ray [27]	Neut. diff. [28]
C1-O5	1.273	1.268	1.262	1.270	1.258	1.260	1.253	1.256	1.265	1.251
C1-O6		1.269	1.283	1.266	1.260	1.257	1.245	1.241	1.243	1.239
C1-C2		1.548	1.535	1.569	1.546	1.567	1.559	1.579	1.534	1.530
C2-N4	1.480	1.471	1.471	1.479	1.466	1.474	1.500	1.507	1.489	1.488
C2-C3		1.549	1.552	1.554	1.544	1.549	1.526	1.521	1.530	1.530
C3-S8	1.862	1.860	1.851	1.872	1.847	1.859	1.833	1.834	1.807	1.800
N4-H7							1.032	1.048	0.840	1.038
N4-H12		1.024	1.024	1.025	1.019	1.020	1.028	1.042	0.970	1.017
N4-H14		1.024	1.022	1.023	1.018	1.018	1.028	1.033	0.980	1.055
C2-H11		1.098	1.095	1.097	1.093	1.093	1.090	1.088	0.940	1.104
C3-H9		1.097	1.097	1.098	1.091	1.091	1.088	1.088		1.077
C3-H10		1.098	1.098	1.100	1.093	1.094	1.090	1.088		1.077
S8-H13							1.363	1.380	1.350	1.270
O5C1O6		125.3	124.0	126.8	125.5	126.9	128.9	129.8	126.6	125.7
O5C1C2	116.7	117.8	119.0	116.6	117.6	116.6	115.7	114.9	118.3	117.3
O6C1C2		116.9	116.9	116.6	116.9	116.4	115.4	115.3	115.7	117.0
C1C2N4	108.9	110.4	110.3	109.9	110.5	110.2	107.9	107.0	108.7	111.1
C1C2C3		108.5	109.5	109.6	108.3	109.5	110.0	111.9	111.5	111.1
C1C2H11		107.6	108.0	107.9	107.5	107.5	110.1	107.6		
H11C2N4		108.2	107.3	108.6	108.5	110.2	107.3	106.3		
C2N4H7							108.0	102.3		
C2N4H12		108.2	106.4	106.4	108.3	106.6	110.8	114.1		
C2N4H14		108.0	108.3	105.0	108.2	105.1	113.2	114.7		
C2C3S8	114.5	114.4	112.5	116.2	114.4	116.1	114.9	117.2	113.7	114.8
C2C3H9		108.5	108.7	107.6	108.5	107.7	107.4	106.5		
C2C3H10		108.5	108.4	107.8	108.5	107.8	111.3	111.2		
C3S8H13							98.1	96.8	90.6	97.0
O5C1C2O6		−177.9	−178.4	−178.5	−177.9	−178.6	−178.4	178.7		
O5C1C2H11		152.9	154.5	151.6	153.1	150.1	134.4	111.3		
O5C1C2N4		35.0	37.6	33.3	34.8	31.4	17.6	−2.6	−35.3	−17.0
C1C2C3S8	−64.9	−175.3	−176.5	177.7	−176.1	177.6	−177.3	−175.9		
C1C2C3H9		−53.7	−54.9	−59.8	−54.3	−59.8	−59.3	−58.5		
C1C2C3H10		62.8	61.8	55.8	62.2	55.9	58.6	58.3		
C2C3S8H13							−93.3	−79.2	80.8	−89.4

Experimental X-Ray and neutron diffraction data are shown for the purpose of comparison. Distances are given in Å and angles in degrees

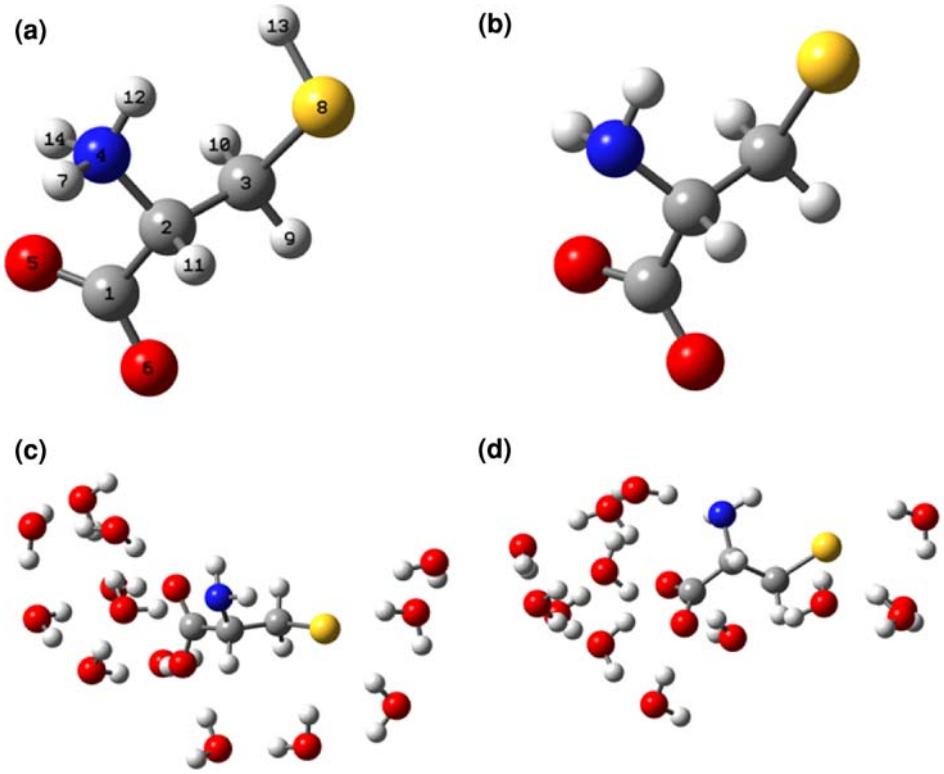

Fig. 2 **a** Gauche conformer considered for cysteine. A second, NCCS anti-conformer, exists but was not considered in this work (numbering of the atoms as used in Table 1). **b** Structure of the dianion of cysteine, deprotonated at both the carboxylic and thiol groups. **c**, **d** Views of the geometry optimized structure of cysteine within a cluster of 13 water molecules

and 0.5 van der Waals 1–4 scale factors, simulation temperature 300 K, 1 ps heat time, 15 ps running time, 1 ps cool time, 10^{-3} ps step size, the nearest 13 molecules out of a stabilized 216 water molecules periodic box were chosen). This structure was further refined through a geometry optimization involving all coordinates at the B3LYP/6-31+G(d) level and further calculation of the IR and Raman spectra.

All calculations were performed using the Gaussian 09 [25] suite of computer programs, in a cluster of Xeon machines. The IR and Rama spectra were plotted using the GausSum 2.1 program [26].

3 Results and discussion

3.1 Cysteine zwitterion and dianion

Table 1 shows the optimum geometries calculated for the zwitterionic Cys and the doubly charged anion, respectively. The theoretical results for the former are compared with the experimental X-ray data of Goerbitz [27] and the neutron diffraction structure obtained by Kerr et al. [28]. In the case of the anion, one sees that the presence of the solvent affects mainly the ionic carboxylate and thiolate groups. In the latter, the C–S distance diminishes when the solvent is simulated using a dielectric and then again when the cluster of water molecules is included. The effect on the carboxylate head is different. While both oxygens are nearly equivalent in the gas-phase structure or when the dielectric is included, the preferential solvation of water through hydrogen bonding makes one of the C–O bonds larger than the other in the cluster. One can appreciate in Fig. 2c the chain of water molecules linking the carboxylate head with the amino group; a chain of importance in the equilibrium between the zwitterion and the anion.

Both oxygens are not equivalent in the zwitterion, in qualitative agreement to the experimental data. One of them is clearly influenced by the interaction with the ammonia group and exhibits a longer bond length both in the experimental and computed structures. The C1–C2 bond is much longer in the gas-phase structure than in the experimental ones, but one appreciates the shortening that occurs when the dielectric field is included. Therefore, it may be concluded that the shorter bond distance is a product of the interactions in the crystal. This may be true also for the C–S bond, although in this case the inclusion of the dielectric field does not produce a shortening. Specific interactions must be playing a role in this case, as was shown for the dianion.

3.2 Vibrational frequencies of the ligands

Vibrational data for the dianion and the zwitterion are presented in Tables 2 and 3, while the spectra are plotted in Fig. 3. We now consider these data. The experimental

Table 2 Vibrational frequencies (in cm^{-1}) and Raman activities (normalized to the activity of the CS frequency) for the cysteine anion

	Experimental		Theoretical										
			S stereoisomer									R stereoisom	
			6-311++G(3df,2pd)				6-31+G(d)				Assignment	6-31+G(d)	
			PCM solvent		Gas phase		PCM solvent		Gas phase			PCM solvent	
	Freq.	Act.	Freq.	Act.	Freq.	Act.	Freq.	Act.	Freq.	Act.		Freq.	Act.
1			98	12	70	23	75	18	69	18	$\tau(CO_2)$	32	6.8
2			120	3.4	117	17	118	3.9	116	2	$\tau(CH_2S)$	126	1.9
3			180	3.6	176	55	182	3.2	178	22	Collective	195	2.1
4	290	8.5	243	3.0	241	13	241	6.8	242	10	$\tau(NH_2)$	221	4.8
5	330	12	266	10	307	11	261	7.0	305	7	$\tau(NH_2)$	273	5.8
6	414	14	336	5.3	386	9.2	333	4.8	385	6	$\tau(NH_2)$	350	7.1
7	541	32	384	4.2	413	52	382	5.9	412	15	$\tau(CH_2S)+ \delta(CCH)$	423	1.6
8	625	33	538	14	533	28	532	17	532	14	$\delta(CH_2S) + \delta(CCH)$	524	12
9	683	100	661	100	649	100	662	100	646	100	$\nu(CS)$	641	10
10			704	56	696	75	704	84	695	51	$\gamma(CO_2) + \delta(CCS) + \nu(CS)$	680	100
11	792	25	812	2.8	802	10	810	15	796	4	$\delta(CCS)$	801	8.2
12	834	33	840	47	829	173	844	67	832	104	$\zeta(CH_2) + \nu(CN)$	843	15
13	911	39	895	106	884	591	898	125	888	321	$\nu(CN) + \nu(CC) + \delta(CNH)$	880	91
14	1,037	16	912	21	933	389	930	32	947	68	$\gamma(NH_2) + \nu(CN)$	933	34
15	1,065	54	1,020	35	1,030	423	1,037	41	1,049	113	$\nu(CC) + \delta(CH_2) + \gamma(NH_2)$	1,001	25
16	1,090	17	1,082	34	1,070	385	1,088	41	1,081	115	$\nu(CN) + \delta(CH_2)$	1,112	17
17	1,151	7.8	1,160	39	1,179	137	1,168	101	1,187	100	$\delta(NCH) + \delta(NH_2)$	1,172	8.7
18	1,203	10	1,206	33	1,203	747	1,219	25	1,218	171	$\delta(HCCH)$	1,248	50
19	1,239	8.6	1,244	7.0	1,230	368	1,262	5.1	1,251	75	$\nu(CN) + \delta(CH_2)$	1,252	8.5
20	1,307	16	1,321	25	1,330	62	1,333	52	1,345	31	$\delta(HCCH)$	1,342	59
21	1,349	33	1,359	107	1,345	361	1,363	160	1,353	187	$\zeta(NH_2) + \nu_s(CO_2) + \nu(CC) + \delta(CCH)$	1,354	22
22	1,413	22	1,412	47	1,386	659	1,424	57	1,403	373	$\gamma(NH_2) + \nu_s(CO_2) + \delta(CCH)$	1,408	46
23	1,428	28	1,463	73	1,462	349	1,483	123	1,484	145	$\gamma(CH_2)$	1,484	67
24	1,567	7.9	1,538	45	1,577	388	1,547	59	1,606	79	$\gamma(NH_2) + \nu_a(CO_2)$	1,545	44
25	1,658	5.2	1,591	26	1,626	221	1,630	40	1,658	50	$\gamma(NH_2)$	1,631	27
26	2,836	16	3,003	1,611	2,985	902	3,022	1,790	3,002	506	$\nu(CH)$	2,922	219
27	2,915	39	3,012	307	3,011	2,184	3,033	634	3,033	560	$\nu_s(CH_2) + \nu(CH)$	3,032	619
28	2,942	36	3,058	634	3,039	612	3,075	812	3,054	377	$\nu_a(CH_2) + \nu(CH)$	3,109	390
29			3,393	1,238	3,389	1,365	3,380	1,420	3,378	942	$\nu_s(NH_2)$	3,406	823
30			3,469	285	3,484	419	3,462	421	3,478	243	$\nu_a(NH_2)$	3,485	273

The data for the *R*-stereoisomer determined in Ref. [11] are also shown

ν stretch, δ deformation, ζ rocking, γ waging, τ torsion, *a* antisymmetric, *s* symmetric

results were obtained by Foley and Enescu [11] in aqueous solution using a pulsed Nd:YAG laser. They used B3LYP/6-31+G(d) calculations as a guide to the assignment of the peaks. Regretfully, they apparently used the *R*-stereoisomer (see Figs. 2, 3 in their paper) for these calculations, instead of the correct L isomer. Although the difference in the spectrum is probably not very large, we repeated their calculations with the B3LYP/6-31+G(d) method on the correct isomer, besides extending them using the much larger 6-311++G(3df,2pd) basis set with the same DFT method.

The general aspect of the vibrational spectra for both species can be gathered from Fig. 3. Both IR spectra are dominated by the symmetric and asymmetric stretching of the CO_2 group, plus the deformation of the ammonia group. In the case of the zwitterion, the different stretching modes of the NH_3 group are noticeable at large frequencies, and these are naturally absent in the spectrum of the dianion (and replaced by the very weak NH_2 bands). Frequencies corresponding to different vibrational modes involving the CH and CH_2 groups are seen as exceedingly

Table 3 Vibrational frequencies (in cm^{-1}) and Raman activities (normalized to the activity of the CS frequency) for the cysteine zwitterion

	Experimental		Theoretical				
			S stereoisomer			*R*-stereoisomer	
			6-311++G(3df,2pd)		Assignment	6-31 + G(d)	
	Freq.	Act.	Freq.	Act.		Freq.	Act.
1			76	6.7	Collective	75	12
2			83	2.3	$\tau(NH_3^+)$	81	8.9
3			95	3.5	Collective	135	3.2
4			163	1.2	$\tau(CH_2SH)$	177	3.4
5	283	29	192	2.5	$\tau(CH_2SH)$	260	3.2
6			244	14.2	Collective	312	3.3
7	345	26	313	11.6	$\tau(CH_2S) + \delta(CCH)$	331	4.5
8	475	19	372	9.0	$\delta(CH_2S) + \delta(CCH)$	484	23
9	529	26	513	8.5	$\delta(CCS)$	505	14
10	622	39	670	2.9	$\gamma(CO_2) + \delta(CCS) + \nu(CS)$	576	29
11	684	100	679	100.0	$\nu(CS)$	666	100
12	780	36	752	2.2	$\zeta(CH_2) + \nu(CN)$	770	55
13	814	25	814	14.3	$\nu(CS) + \nu(CC) + \delta(CCC)$	790	9.8
14	875	34	858	86.8	$\gamma(NH_3^+)+\nu(CN)$	850	34
15	935	30	888	22.4	$\nu(CC) + \delta(CH_2) + \gamma(NH_3^+)$	905	31
16	994	19	961	13.0	$\nu(CN) + \delta(CH_2)$	977	34
17	1,064	20	1,033	19.5	$\delta(NCH) + \delta(NH_3^+)$	1,061	8.7
18	1,115	16	1,079	647.2	$\delta(HCCH)$	1,074	12
19	1,140	17	1,133	6.1	$\zeta(NH_3^+)+\nu_s(CO_2^-) + \nu(CC) + \delta(CCH)$	1,119	23
20	1,213	21	1,229	65.4	$\delta(HCCH_2)$	1,238	90
21	1,276	14	1,268	78.4	$\delta(HCCH_2)$	1,301	14
22	1,311	26	1,313	59.1	$\delta(HCCH_2)$	1,330	17
23	1,345	46	1,358	68.3	$\nu(CC) + \delta(NCH)$	1,369	52
24	1,390	43	1,393	18.9	$\nu(CC) + \delta(NCH)$	1,398	50
25	1,430	35	1,449	23.2	$\gamma(CH_2)$	1,461	38
26	1,513	9.7	1,454	16.7	$\gamma(NH_3^+)$	1,475	38
27	1,614	18	1,575	18.6	$\delta(NH_3^+)$	1,595	63
28	1,647	14	1,627	29.5	$\delta(NH_3^+)$	1,644	49
29			1,634	26.3	$\gamma(NH_2) + \nu_a(CO_2)$	1,657	22
30	2,581	61	2,371	960.4	$\nu(SH)$	2,412	1,198
31	2,837	10	3,043	878.1	$\nu_s(CH_2) + \nu(CH)$	3,013	934
32	2,959	58	3,058	179.6	$\nu_s(CH_2)$	3,074	890
33	3,001	31	3,116	262.3	$\nu_a(CH_2)$	3,148	448
34			3,262	506.6	$\nu_s(NH_3^+)$	3,262	762
35			3,322	255.1	$\nu_{a1}(NH_3^+)$	3,308	102
36			3,351	162.3	$\nu_{a2}(NH_3^+)$	3,348	271

ν stretch, δ deformation, ζ rocking, γ waging, τ torsion, *a* antisymmetric, *s* symmetric

weak signals in both the zwitterion and dianionic spectra. The Raman spectra of both species are distinguishable by the presence or lack of the S–H signal calculated at 2,371 cm^{-1} (PCM/B3LYP/6-311++G(3df,2dp) level) and measured at 2,581 cm^{-1} according to Foley and Enescu [11] and 2,540 cm^{-1} by Pawlukojć et al. [29]. The large discrepancy between the theoretical and experimental result (ca. 200 cm^{-1}) is probably due to the lack of anharmonicity and specific interactions (hydrogen bonding) in the calculations.

There is a striking and troublesome difference between the theoretical and experimental results for the cysteine

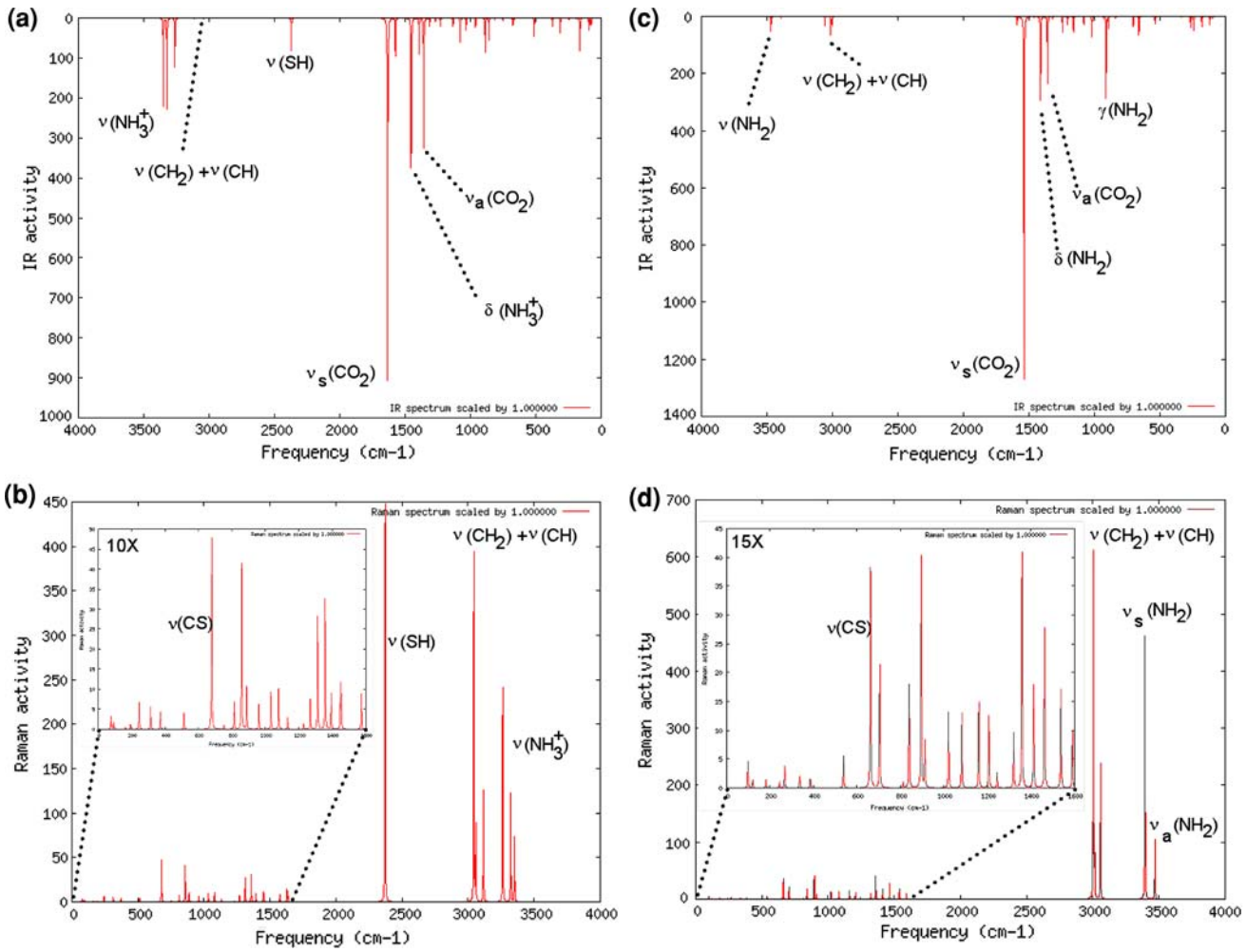

Fig. 3 IR (**a**) and Raman (**b**) spectra of the cysteine zwitterion, and IR (**c**) and Raman (**d**) spectra of the cysteine dianion calculated at the PCM/B3LYP/6-311++G(3df,2pd) level; the zone between 0 and 1,600 cm^{-1} has been blown up to allow better appreciation of the details

zwitterion. According to the results of Foley and Enescu [11] the dominant band in the Raman spectrum should be the C–S vibration, with the SH stretching/deformation and the CH_2 symmetric stretching being about half as active as the former. Pawlukojć et al. [29] did not publish values for the relative activities, but from their Fig. 5 for the Raman spectrum for normal and deuterated L-Cys one can see that the activities of the three bands are almost equal. The B3LYP/6-31+G(d) calculations by Foley and Enescu [11] tell a completely different story, with the SH and CH_2 bands being about 10–12 times stronger than the CS one. They attribute this discrepancy to wrongly calculated activities in the high and low frequency regions due to the difficulty in the evaluation of the third derivatives needed to calculate the Raman activities. They assume that the use of larger basis sets would correct this mistake [30], but our own calculations with a much larger basis set of similar accuracy to those performed by Halls and Schlegel in their benchmark calculations show exactly the same behavior as with the smaller basis set, although the ratio is little smaller (9.6 against 12.0). A perusal of the available bibliography did not afford any hint about previous calculations that reported any similar discrepancy, so that for the moment this has to be regarded as an unaccounted failure of the theoretical calculations. One of the reviewers pointed out that these discrepancies could be explained also considering anharmonic corrections as seen for the OH and NH bonds in the case of the formamide–water and formamide–formamide systems [31]. Other reviewer pointed out that the discrepancy might be due to the presence of different conformers, as observed in [32]. Further research is being done on simpler systems involving the SH group to try to understand this issue.

The effect of the solvent in the Raman spectrum of the anion was studied comparing the gas-phase spectrum with those obtained in solution through two approximate models. As reported in the Sect. 2, the first model implied a full geometry optimization of the anion in the dielectric, and

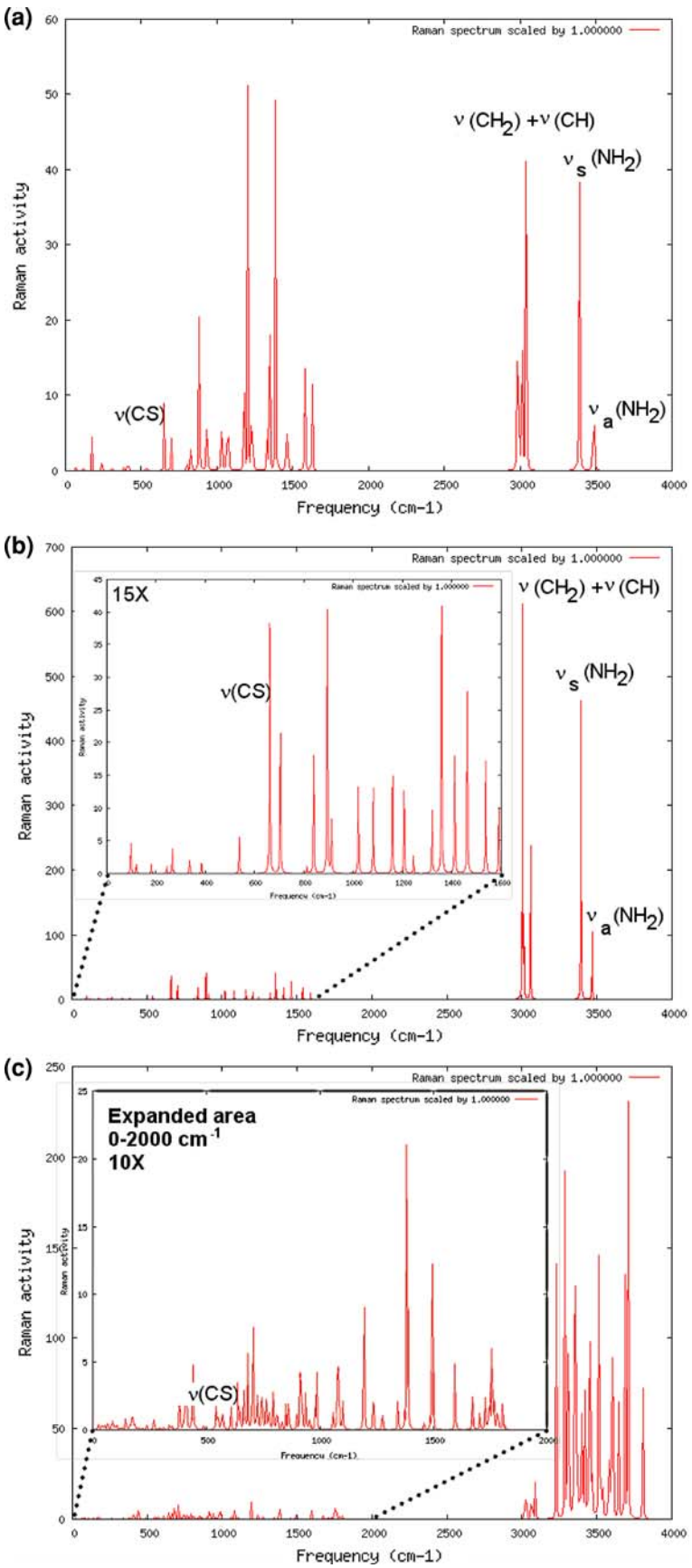

Fig. 4 Comparison of the Raman spectra of the cysteine dianion calculated **a** in gas phase, **b** simulating a water solvent using the PCM method, and **c** in a cluster with 13 water molecules. The zone between 0 and 1,600 cm^{-1} has been expanded in **b** and **c** to better appreciate the details. Notice the difference in the scales employed

was performed starting from the gas-phase geometry and using the PCM method to include the solute into a cavity surrounded by polarized charges. The second model consisted in a cluster of 1 anion molecule and 13 water molecules chosen from those belonging to the first and second solvation sphere, as obtained from a classical molecular dynamics simulation. The cluster was fully geometry optimized and the Raman spectrum of the whole system calculated in the same way as before. The results of the three approximations are shown in Fig. 4.

The solvent induces a very small shift in the position of the bands, but a noticeable modification of the relative intensities of the ν(CS) and ν(CH), $\nu(CH_2)$ and $\nu(NH_2)$ bands. The inclusion only of the polarization field, through the PCM method, increases markedly the activity of the latter bands with respect to the former, but the inclusion of discrete water molecules moderates this increase greatly, especially in what concerns the CH and CH_2 stretchings. The NH_2 stretching is masked by the OH stretchings of the water molecules and we assume this is the reason they are not reported in the experimental spectrum of Foley and Enescu [11].

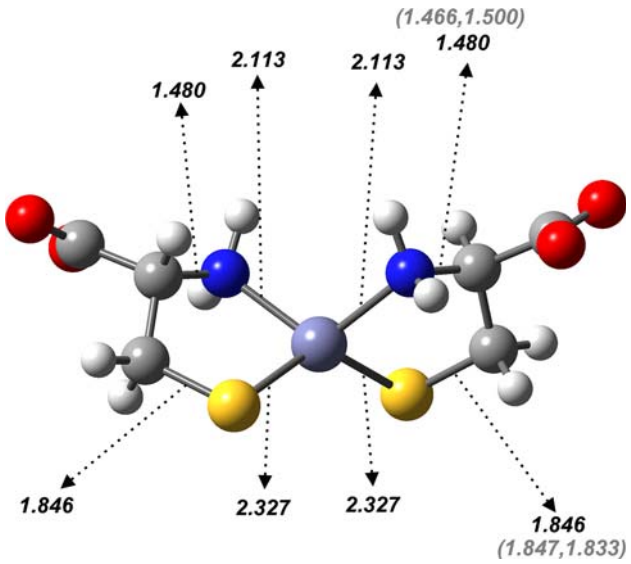

Fig. 5 B3LYP/6-311++G(3df,2pd) optimum structure of the $Zn(Cys)_2$ complex. Symmetry was not imposed on the complex but obtained as a result of the optimization process. Bond lengths are in Å. The values in parenthesis are the lengths of the CN and CS bonds in the zwitterion and the anion, respectively

3.3 The $(Cys)_2Zn$ complex

An initial optimization at the B3LYP/6-31G(d) level was attempted at the structure described by Foley and Enescu. This structure has two problems: the first one is that, as we mentioned before, one of the cysteine residues is the L-Cys enantiomer, while the other is the *R*-Cys enantiomer. Therefore, this cannot be the structure of the actual complex. Moreover, it is well-known that Zn(II) forms tetracoordinated tetrahedral complex, with pentacoordination occurring rarely. But it almost never appears as hexacoordinated. Finally, the structure described by Foley and Enescu is not stable as such, unless one fixes artificially the symmetry of the compound, requesting opposing Zn–N, Zn–O and Zn–S bond lengths to be equal.

For only the purpose of comparison, the initial structure obtained in Ref. [11] was reoptimized but allowing all geometrical parameters to vary. Since the purpose was only to test the reported structure, only the smaller basis set was employed (B3LYP/6-31+G(d) method). The optimum structure shows the expected preference of sulfur bonding to Zn, since the Zn–S bond lengths decrease considerably with respect to the optimum structure with imposed symmetry. One of the Zn–N bonds remains approximately the same, while the other elongates considerably, and one of the Zn–O bonds simply breaks. The optimum (L-Cys)(*R*-Cys)Zn(II) complex is then pentacoordinated, while the non-bonded COO group prefers to hydrogen bond to NH_2 instead of coordinating the Zn atoms. The optimum structure then is not hexacoordinated, even if the wrong stereoisomer is included in the complex.

The actual minimum for $(L\text{-Cys})_2Zn(II)$ optimized at the B3LYP/6-311++G(3df,2pd) level including the PCM modeling of the solvent, is depicted in Fig. 5. The complex is actually tetracoordinated and tetrahedral, both COO groups do not participate in the bonding to the metal. Geometry optimization was performed without imposing any symmetry restriction. Even so, the final geometry turns out to be very symmetrical, with both Cys chelating identically as shown by the Zn–S and Zn–N distances to both the A and B fragments. We also show in the figure the optimum CN and CS distances, at the same level of calculation, for the zwitterion and the anion. One sees that the CN bond is closer to that in the anion than in the zwitterion, while the opposite occurs with the CS bonds.

3.4 Vibrational frequencies of the complex

The experimental and vibrational frequencies for the complex are collected in Table 4 and depicted in Fig. 6. One sees that there is an almost perfect agreement between the experimental and theoretical vibrational frequencies. As was the case with the ligands, the C–H and N–H vibrations exhibit a much larger Raman activity than the C–S vibration. The NH_2 vibrational frequencies are not reported in the experimental spectrum but, as we showed before, this is the zone where the OH vibrations of the solvent water molecules appear, which may explain this fact. It may also be that they appear outside the range

Table 4 Vibrational frequencies (in cm^{-1}) and Raman activities (normalized to the activity of the CS frequency) for the complex

	Experimental		Ref. [11]		Our work		Assignment
			B3LYP/6-31 + G(d)		B3LYP/6-311++G(3df,2pd)		
	Freq.	Act.	Freq.	Act.	Freq.	Act.	
1	296	119	316	14	249	12	$\nu_s(S_A\text{-}Zn\text{-}S_B)$
2					273	4	$\nu_a(S_A\text{-}Zn\text{-}S_B)$
3	334	118	383	27	319	61	δ(CCS-Zn-SCC)
4					325	4	δ(CCS-Zn-SCC)
5					348	16	δ(NCS-Zn-SCN)
6					352	3	δ(NCS-Zn-SCN)
7	399	61	420	14	444	3	$\nu_s(N_A\text{-}Zn\text{-}N_B)$
8					447	1	$\nu_a(N_A\text{-}Zn\text{-}N_B)$
9					518	0	$\gamma(NH_2)_A - \gamma(NH_2)_B$
10	532	38	560	16	526	4	$\gamma(NH_2)_A + \gamma(NH_2)_B$
11	569	39	588	6	571	0	$\delta(N_A\text{-}Zn\text{-}N_B)$
12					597	5	$\tau(CNH_2)_A + \tau(CNH_2)_B$
13	685	100	653	100	673.6	12	$\nu(CS)_A - \nu(CS)_B$
14					673.8	100	$\nu(CS)_A + \nu(CS)_B$
15					711	9	$\delta(CCO_2)_A + \delta(CCO_2)_B$
16					712	3	$\delta(CCO_2)_A - \delta(CCO_2)_B$
17	805	28	799	43	811	5	$\gamma(CO_2)_A + \delta(CCC)_A + \nu(CS)_A$
18					811	5	$\gamma(CO_2)_B + \delta(CCC)_B + \nu(CS)_B$
19	849	21	864	15	849	5	$\tau(CCH_2)_A$
20					849	22	$\tau(CCH_2)_B$
21	920	3	911	11	906	76	$\nu(C\text{-}CO_2)_A + \nu(C\text{-}CO_2)_B$
22					907	20	$\nu(C\text{-}CO_2)_A - \nu(C\text{-}CO_2)_B$
23	968	19	953	26	961	3	$\nu(C\text{-}CH_2)_A + \nu(C\text{-}CH_2)_B$
24					962	10	$\nu(C\text{-}CH_2)_A - \nu(C\text{-}CH_2)_B$
25	1,058	20	1,067	25	1,052	1	$\nu(C\text{-}NH_2)_A + \nu(C\text{-}NH_2)B$
26					1,053	27	$\nu(C\text{-}NH_2)_A - \nu(C\text{-}NH_2)_B$
27					1,109	0.7	$\gamma(CH_2)_A + \gamma(CH_2)_B$
28					1,110	5	$\gamma(CH_2)_A - \gamma(CH_2)_B$
29	1,190	16	1,162	32	1,137	9	$\delta(HCNH_2)_A - \delta(HCNH_2)_B$
30					1,138	1	$\delta(HCNH_2)_A + \delta(HCNH_2)_B$
31	1,218	13	1,194	53	1,231	6	$\delta(HCCH_2)_A + \delta(HCCH_2)_B + \zeta(NH_2)_A + \zeta(NH_2)_B$
32					1,231	6	$\delta(HCCH_2)_A - \delta(HCCH_2)_B + \zeta(NH_2)_A - \zeta(NH_2)_B$
33	1,256	14	1,280	51	1,267	2	$\delta(HCCH_2)_A + \delta(HCCH_2)_B - \zeta(NH_2)_A - \zeta(NH_2)_B$
34					1,268	15	$\delta(HCCH_2)_A + \delta(HCCH_2)_B + \zeta(NH_2)_A + \zeta(NH_2)_B$
35	1,301	23	1,336	44	1,305	18	$\delta(HCCH_2)_A + \delta(HCCH_2)_B$
36					1,305	62	$\delta(HCCH_2)_A - \delta(HCCH_2)_B$
37	1,355	24	1,345	45	1,368	7	$\delta(HCN)_A - \delta(HCN)_B + \zeta(NH_2)_A - \zeta(NH_2)_B + \nu(CCO_2)_A - \nu(CCO_2)_B$
38					1,369	52	$\delta(HCN)_A - \delta(HCN)_B + \zeta(NH_2)A - \zeta(NH_2)_B + \nu(CCO_2)_A - \nu(CCO_2)_B$
39	1,405	31	1,419	72	1,404	23	$\delta(HCN)_A - \delta(HCN)_B + \zeta(NH_2)_A - \zeta(NH_2)_B + \nu(CCO_2)_A - \nu(CCO_2)_B$
40					1,404	18	$\delta(HCN)_A - \delta(HCN)_B + \zeta(NH_2)_A - \zeta(NH_2)_B + \nu(CCO_2)_A - \nu(CCO_2)_B$
41	1,433	22	1,492	69	1,471	1	$\delta(CH_2)_A - \delta(CH_2)_B$
42					1,471	13	$\delta(CH_2)_A + \delta(CH_2)_B$

Table 4 continued

	Experimental		Ref. [11]		Our work		Assignment
			B3LYP/6-31 + G(d)		B3LYP/6-311++G(3df,2pd)		
	Freq.	Act.	Freq.	Act.	Freq.	Act.	
43	1,596	15	1,592	41	1,574	29	$\delta(HCCO_2)_A + \delta(HCCO_2)_B + \delta(CO_2)_A + \delta(CO_2)_B$
44					1,574	7	$\delta(HCCO_2)_A - \delta(HCCO_2)_B + \delta(CO_2)_A - \delta(CO_2)_B$
45	1,659	12	1,639	26	1,607	7	$\delta(NH_2)_A - \delta(NH_2)_B$
46					1,608	8	$\delta(NH_2)_A + \delta(NH_2)_B$
47	2,851	10	3,012	1,162	3,024	246	$\nu(CH)_A - \nu(CH)_B + \nu_s(CH_2)_A - \nu_s(CH_2)_B$
48					3,024	998	$\nu(CH)_A + \nu(CH)_B + \nu_s(CH_2)_A + \nu_s(CH_2)_B$
49	2,930	38	3,036	1,464	3,040	103	$\nu(CH)_A + \nu(CH)_B - \nu_s(CH_2)_A - \nu_s(CH_2)_B$
50					3,040	62	$\nu(CH)_A - \nu(CH)_B - \nu_s(CH_2)_A + \nu_s(CH_2)_B$
51	2,967	26	3,090	662	3,099	160	$\nu_a(CH_2)_A + \nu_a(CH_2)_B$
52					3,099	406	$\nu_a(CH_2)_A - \nu_a(CH_2)_B$
53			3,350	1,207	3,349	18	$\nu_s(HNH)_A - \nu_s(HNH)_B$
54					3,350	765	$\nu_s(HNH)_A + \nu_s(HNH)_B$
55			3,427	478	3,402	96	$\nu_a(HNH)_A - \nu_a(HNH)_B$
56					3,403	197	$\nu_a(HNH)_A + \nu_a(HNH)_B$

Experimental and theoretical data from Ref. [11] are shown for comparison purposes

ν stretch, δ deformation, ζ rocking, γ waging, τ torsion, *a* antisymmetric, *s* symmetric, A and B are the Cys substituents

accessible for the experimental setup of Foley and Enescu. We do not have an explanation for the difference between the experimental and theoretical data concerning the activities of the NH vibrations.

The second fact to be pointed out is that the Zn–N stretchings are clearly appreciated at 444/447 cm^{-1} theoretically and 399 cm^{-1} experimentally. The same happens for the Zn–S stretchings which appear at 249 (symmetric) and 273 (antisymmetric) cm^{-1} theoretically and 296 cm^{-1} experimentally. Differently from the conclusion by Foley and Enescu, we found a small mode mixing in these bands. The rest of the ligand body somehow participates in the movement, but not in the significant way predicted in Ref. [11] due to the wrong structure employed for the calculations.

The complex exhibits two bands in the region 1,500–1,700 cm^{-1} which are clearly attributable to the CO_2 asymmetrical stretching and the NH_2 angular vibrations. We found these bands at 1,574 and 1,607 cm^{-1} in good agreement with the experimental data (1,596 and 1,659 cm^{-1}). Ikram and Powell [33], who studied the IR spectrum of solid $Zn(Cys)_2$, found these bands at 1,580 and 1,615 cm^{-1} in even better agreement with our theoretical results.

The case for O coordination manifesting in the experimental spectrum was constructed by the supposed appearance of the CO_2 rocking vibration at 399 cm^{-1}, a vibration absent both in the zwitterion and the anion, and therefore attributable to coordination. However, our calculation shows that this experimentally measured band is actually the stretching of the Zn–N bonds. Thus, there is no experimental support for hexacoordination, in agreement with our theoretical results on the structure of the complex.

4 Conclusions

The structure of the zwitterion and anion of Cys, as well as the Zn(Cys) complex have been studied at the density functional level, using the B3LYP method and the 6-31+G(d) and 6-311++G(3df,2pd) basis sets. Water acting as the solvent was simulated employing a polarizable dielectric according to the PCM method. The results show clearly that the optimum structure of the complex is tetracoordinated and tetrahedral, not hexacoordinated and octahedral as previously proposed. There is only Zn–N and Zn–S coordination in the complex; the COO groups are free from the interaction with the Zn atom. The octahedral structure proposed previously is only an artefact produced by imposing artificial symmetry constraints and considering the wrong stereoisomer.

Raman spectra of the three species were calculated. It is shown that the calculated vibrational spectra of the complex agree well with the experimental results. The analysis of the simulated Raman spectrum shows the presence of bands attributable to Zn–N and Zn–S bonds at 249/273 and 444/447 cm^{-1}, in reasonable agreement with the experimental results (296 and 399 cm^{-1}). The experimental band

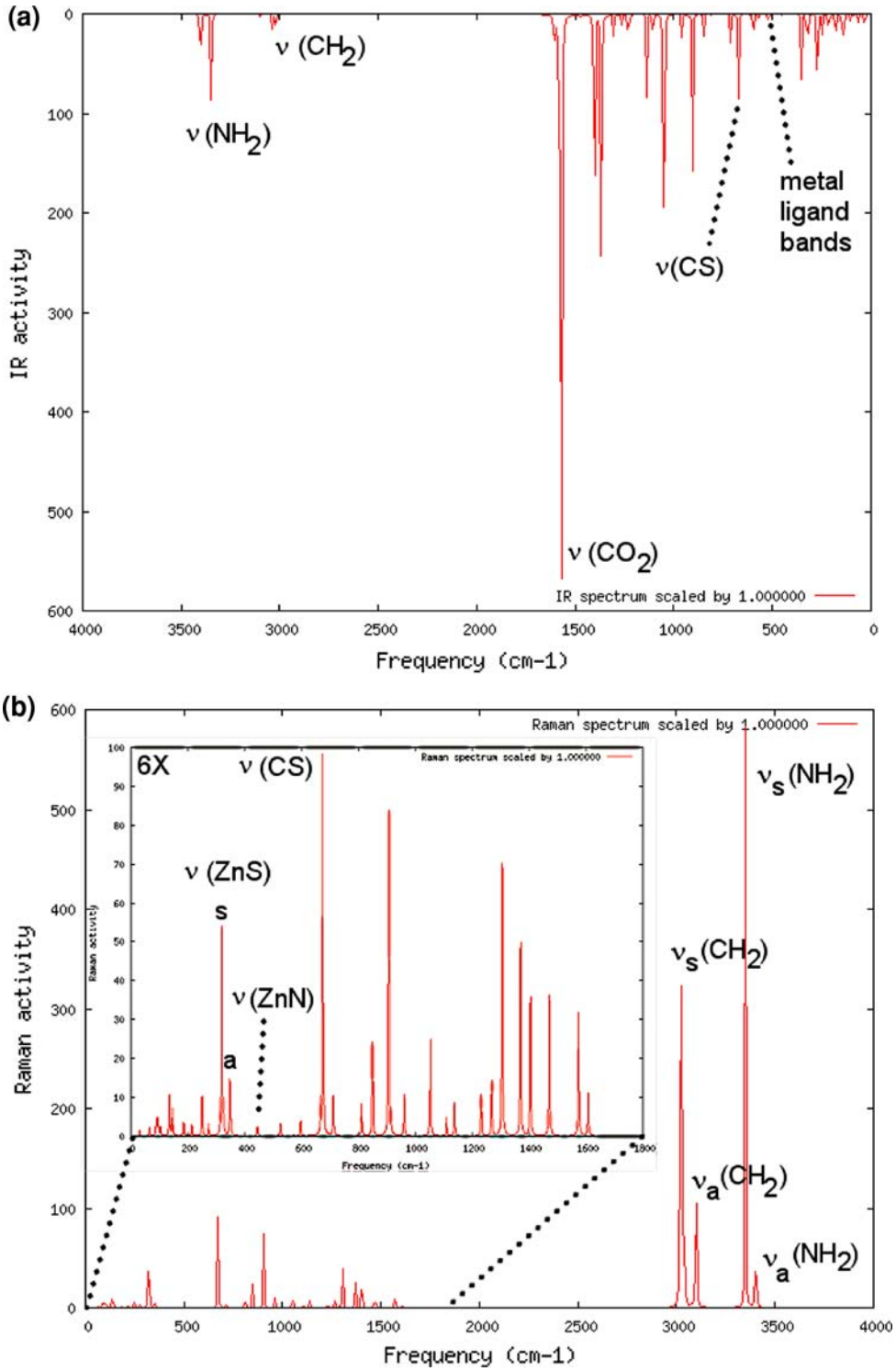

Fig. 6 **a** IR and **b** Raman simulated spectra [at the PCM/B3LYP/6-311++G(3df,2pd) level] of the equilibrium structure of the $(Cys)_2Zn^{2-}$ complex. The region between 0 and 1,600 cm^{-1} was expanded as in the previous figures

at 334 cm^{-1} is indeed an amino acid–metal band with large contributions from the skeletal movements of the ligand. This band was wrongly assigned in Ref. [11], the same as the experimental band at 399 cm^{-1} (here theoretically determined to be 444 cm^{-1}) which was assumed to represent the CO_2^- rocking (here a metal–ligand band, see Table 4). The correct assignment, however, shows that there are two specific metal–ligand bands, slightly contaminated by ligand internal vibrations, and another metal–ligand band with heavy contamination. Of course, none of them involves metal–oxygen bonding, since the CO_2^- fragments are pointing away from the metal.

Acknowledgments This work was performed under the auspices of Pedeciba Química (PNUD Proy. URU/06/004) and PDT 63/350. We gratefully acknowledge Professor and friend Sándor Suhai for his generous hospitality and discussions about our research.

References

1. Klug A, Schwabe W (1995) FASEB J 9:597
2. Wolfe SA, Grant RA, Elrod-Erickson M, Pabo CO (2001) Structure (Camb) 9:717
3. Laity JH, Lee BM, Wright PE (2001) Curr Opin Struct Biol 11:39
4. Leon O, Roth M (2000) Biol Res 33:21
5. Gamsjaeger R, Liew CK, Loughlin FE, Crossley M, Mackay JP (2007) Trends Biochem Sci 32:63
6. Iuchi S (2001) Cell Mol Life Sci 58:625
7. Maeder ML, Thibodeau-Beganny S, Osiak A, Wright DA, Anthony RM, Eichtinger M, Jiang T, Foley JE, Winfrey RJ, Townsend JA, Unger-Wallace E, Sander JD, Müller-Lerch F, Fu F, Pearlberg J, Göbel C, Dassie JP, Pruett-Miller SM, Porteus MH, Sgroi DC, Iafrate AJ, Dobbs D, McCray PB Jr, Cathomen TI, Voytas DF, Keith Joung J (2008) Mol Cell 31:294
8. Shindo H, Brown TL (1965) J Am Chem Soc 87:1904
9. Gockel P, Vahrenkamp H, Zuberbühler AD (1993) Helv Chim Acta 76:511
10. Gockel P, Vogler R, Vahrenkamp H (1996) Chem Ber 129:887
11. Foley S, Enescu M (2007) Vib Spectrosc 44:256
12. Becke AD (1993) Chem Phys 98:5648
13. Lee C, Yang W, Parr RG (1988) Phys Rev 98:785
14. Adamo C, Barone V (1999) J Chem Phys 110:6158
15. Deng Z, Polavarapu PL, Ford SJ, Hecht L, Barron LD, Ewig CS, Jalkanen K (1996) J Phys Chem 100:2025
16. Jalkanen KJ, Suhai S (1996) Chem Phys 208:81
17. Han W-G, Jalkanen KJ, Elstner M, Suhai S (1998) J Phys Chem B 102:2587
18. Poon C-D, Samulski ET, Weise CF, Weisshaar JC (2000) J Am Chem Soc 122:5642
19. Weise CF, Weisshaar JC (2003) J Phys Chem A 107:3265
20. Deplazes E, van Bronswijk, Zhu WF, Barron LD, Ma H, Nafie LA, Jalkanen KJ (2008) Theor Chem Acc 119:155
21. Mukhopadhyay P, Zuber G, Beratan DN (2008) Biophys J 95:5574
22. Losada M, Xu Y (2007) Phys Chem Chem Phys 9:3127
23. Jalkanen KJ, Degtyarenko IM, Nieminen RM, Cao X, Nafie LA, Zhu F, Barron LD (2008) Theor Chem Acc 119:191
24. Cossi M, Scalmani G, Rega N, Barone V (2002) J Chem Phys 117:43
25. Gaussian 09, Revision A.1, Frisch MJ, Trucks GW, Schlegel HB, Scuseria GE, Robb MA, Cheeseman JR, Scalmani G, Barone V, Mennucci B, Petersson GA, Nakatsuji H, Caricato M, Li X, Hratchian HP, Izmaylov AF, Bloino J, Zheng G, Sonnenberg JL, Hada M, Ehara M, Toyota K, Fukuda R, Hasegawa J, Ishida M, Nakajima T, Honda Y, Kitao O, Nakai H, Vreven T, Montgomery JA Jr, Peralta JE, Ogliaro F, Bearpark M, Heyd JJ, Brothers E, Kudin KN, Staroverov VN, Kobayashi R, Normand J, Raghavachari K, Rendell A, Burant JC, Iyengar SS, Tomasi J, Cossi M, Rega, Millam NJ, Klene M, Knox JE, Cross JB, Bakken V, Adamo C, Jaramillo J, Gomperts RE, Stratmann O, Yazyev AJ, Austin R, Cammi C, Pomelli JW, Ochterski R, Martin RL, Morokuma K, Zakrzewski VG, Voth GA, Salvador P, Dannenberg JJ, Dapprich S, Daniels AD, Farkas O, Foresman JB, Ortiz JV, Cioslowski J, Fox DJ (2009) Gaussian, Inc., Wallingford, CT
26. O'Boyle NM, Tenderholt AL, Langner KM (2008) J Comp Chem 29:839
27. Goerbitz CH, Dalhus B (1996) Acta Crystallogr C 52:1756
28. Kerr KA, Ashmore JP, Koetzle TF (1975) Acta Crystallogr B 31:2022
29. Pawlukojć A, Leciejewicz J, Ramirez-Cuesta AJ, Nowicka-Scheibe J (2005) Spectrochim Acta A 61:2474
30. Halls M, Schlegel B (1999) J Chem Phys 111:8819
31. Bende S, Suhai S (2005) Int J Quantum Chem 103:841
32. Jalkanen KJ, Nieminen RM, Frimand K, Bohr J, Bohr H, Wade RC, Tajkhorshid E, Suhai S (2001) Chem Phys 265:125
33. Ikram M, Powell DB (1973) Pak J Sci Res 25:53